Chapter 5

Fluorescence Properties of Rare-Earth-Doped Sol-Gel Glasses

Helena Cristina Vasconcelos and Afonso Silva Pinto

Additional information is available at the end of the chapter

http://dx.doi.org/10.5772/intechopen.68534

Abstract

Glasses may be prepared by sol-gel processing over a wide range of compositions and thick multilayer deposits may be used as waveguides for integrated optics. Doping these layers with rare-earth (RE) ions enables the fabrication of active devices for optical amplifiers; the incorporation of these ions into nanocrystallites offers possibilities for increased dopant concentration without fluorescence quenching, improved spectroscopic performance and high quantum yields. Rare-earth (RE) ions such as erbium (Er^{3+}), ytterbium (Yb^{3+}), neodymium (Nd^{3+}), thulium (Tm^{3+}), holmium (Ho^{3+}) and praseodymium (Pr^{3+}) have been widely used in optical applications and cover a range of wavelengths ranging from UV-visible to the near infrared. This chapter includes basic principles of fluorescence in RE doped glasses, fluorescence lifetimes, quantum yields and Judd-Ofelt analysis. A few information is given about the preparation and characterization of glasses, thin films and glass-ceramics (nanocrystallites embedded in glass matrix) prepared by sol-gel processing. The growth of nanocrystals in glassy sol-gel films through suitable heat treatments can avoid the influence of high phonon energy of silica glasses. The characterization of such materials can be evaluated by optical techniques, namely UV-Visible, FTIR, among other additional techniques that include Scanning Electron Microscopy (SEM), X-ray Diffraction (XRD) and Atomic Force Microscopy (AFM).

Keywords: sol-gel, rare earths, fluorescence, glass, nanocrystallites

1. Light, glasses, and rare earths

The need for high-speed data associated with the advance of telecommunication systems by optical transmission and fiber-optic connections has contributed to extend the optical regime

to integrated circuits [1]; currently, waveguides and other devices necessary for a suitable operation of integrated optical circuits in transmission systems are increasingly being investigated. In the past, coaxial (electrical) cables were used for analog and digital signal transmission over long-distance communications. But the strong attenuation of the signal (about 30 dB/km at 400-MHz cable) [2] imposed the use of regenerative repeaters along the entire route. Fiber optic is now an easy way to transmit information, and the next generation of long-range communications will rely on optical amplifiers to the detriment of regenerative electronic repeaters. The discovery of new glasses of exceptional optical transparency and reduced attenuation to values lower than 1 dB/km boosted the great evolution of optical communication over the last years. Inorganic glasses have been used as optical materials for a long time due mainly to its high transparency in the visible and adjacent, ultraviolet (UV) and near-infrared (NIR) ranges. However, they do not exhibit electronic transitions in this region. For these transitions to take place, controlled introduction of optically active ions is used; therefore, the optical properties of rare-earth (RE) ion-doped inorganic glasses emerged in the field of materials physics. New optical materials suitable for the development of photonic devices based on RE-doped crystal or glassy hosts have thus attracted significant scientific and technological interest. Such wide technological applications are based on the interaction of light with matter where the fluorescent behavior is essential [3]. The most widely used RE ions in glass are erbium (Er^{3+}) [3], ytterbium (Yb^{3+}), and neodymium (Nd^{3+}). For instance, Er^{3+}-doped silica fiber is extensively used in optical communication; Yb^{3+}-doped silica fiber is used in engineering materials processing, and Nd^{3+} doped is applied in glass lasers used for inertial confinement fusion (ICF). The invention of erbium (Er^{3+})-doped fiber optic amplifiers in 1987, the so-called EDFA's, "*Erbium-Doped Fiber Amplifiers*" [3, 4], allowed the optical amplification of the signal around 1550 nm, the region where the propagation of light in silica (SiO_2) optical fibers is maximum, by using stimulated emission of optically excited Er^{3+} ions through transitions from the $^4I_{13/2}$ metastable energy level to the $^4I_{15/2}$ ground state. Furthermore, in integrated optical circuits, which are the equivalent optical of the electronic-integrated circuits ("*chips*"), the light is confined and routed to different optical components (lasers, electro-optical modulators, directional couplers, filters and multiplexers, etc.) through passive devices as *optical planar* (or slab) *waveguides* [3, 4]. A *slab* waveguide is similar to an optical fiber, except that it is a planar, rather than cylindrical. The transmission of light over slab waveguide is possible when a low refractive index glassy contains a slab (or channel) of higher index material, along which light is guided by total internal reflection. These devices can be easily prepared, for example, by sol-gel [5], in different shapes and sizes with uniform distribution of RE ion concentrations, without inducing crystallization, and exhibit large optical transparency window covering UV, visible, and IR regions. In particular, planar optical waveguides, as well as waveguides of different geometry channels, are currently manufactured in materials such as SiO_2 (silica-on-silicon) [5], Si (silicon-on-insulator) [6], GaAs, and $LiNbO_3$ [7]. In the field of photonics, silica-on-silicon technology stands out, where silica glass waveguides are manufactured on silicon substrates, allowing the combination of some discrete optical components with integrated ones [3]. Silica-on-silicon-integrated optical devices can be widely prepared by several methods, such as sputtering, silicon thermal oxidation, flame hydrolysis deposition (FHD), chemical vapor deposition (CVD), and sol-gel spin-coating and/or dip-coating [5]. The future of integrated optics therefore depends on the development of active

(doped) materials signal amplification applications (e.g., optical amplifiers at 1550 nm, wavelength of great interest in fiber optic communications) [4], as well as materials with *passive* performance for the functions of detection, conduction, multiplexing, and de-multiplexing of optical signals, including ultra-fast switches, with response times on the order of picoseconds [8]. Silica-on-silicon passive devices have been highly developed, for instance by NTT (Japan) [9] using FHD. Presently, an alternative technique is sol-gel deposition, in which a liquid precursor is deposited and annealed to form the glass [10]. This process does not require high cost with respect to equipment, is environmentally tolerable, and is highly versatile in the control of final composition and microstructure. This advantage allows diverse modifications to the host glass and the addition of a wide variety of dopants, thus greatly increasing the range of applications of the resulting components. In fact, doping is an important technique used for the development of optical materials, by combining properties of a matrix (the host) with the dopant ones to give an "optical material" of unique properties. In both the cases of 1550-nm amplification and ultra-fast switching, the matrix used is generally a dielectric and the dopant introduced depends on the nature of the application. Thus, in the field of optical amplification, thulium (Tm^{3+}), holium (Ho^{3+}), and praseodymium (Pr^{3+}) have been accommodated by many simple and multicomponent glass matrices [3], displaying several spectroscopic properties, namely radiative transitions between energy levels that cover the UV, visible, and NIR spectral range. Rather, in the case of ultra-fast switching, it is worth noting the doping with metallic nanoparticles (Au, Ag, Cu, etc.), because they have excellent properties in nonlinear optics [11]. Over the past few decades, glasses have provided technological support for the spectrum of needs in optical and photonic applications, especially as host matrices. Glass-integrated optics is dominated by oxide glasses mainly due to its superior production techniques. SiO_2 glasses are of superior significance due to their application in actual optical fibers. These applications have also seriously increased the development of appropriate sources of pumping to meet the demands of the expanding field of communications. Diode lasers with 800- and 980-nm emissions [12] were developed because they coincide with electron transitions of Nd^{3+} and Er^{3+} ions, respectively. Since the discovery of the laser action in a glass-hosted Nd^{3+} ions [13], the study of RE ion-doped glasses has developed enormously, especially in order to obtain (1) new transitions at different wavelengths, (2) new host glasses suitable for the miscibility of RE, and (3) new pump conditions from compact lasers capable of integration for applications in photoluminescence and amplification. The low solubility of RE in silica glass [3] leads to a possible formation of RE clusters, mostly if the doping concentration is higher than the equilibrium solubility. This phenomenon is particularly complex in integrated optical amplifiers since they need a much higher Er^{3+} concentration with respect to EDFAs in order to compensate the smaller interaction length. This high dopant concentration is also responsible for parasite effects caused by interactions between excited ions, notably cooperative up-conversion (UC) and quenching by energy transfer [3, 14], which is detrimental to the optical properties of laser glasses. Special actions are needed to suppress RE clustering. A promising approach is to add suitable network modifiers to SiO_2, such as Al_2O_3 and P_2O_5, in order to improve the RE solubility [15, 16]. The performances of the amplifier are governed by the electronic and optical characteristics of the RE ion but are also strongly influenced by matrix properties. Moreover, the matrix phonon energy is a crucial aspect, because it affects the amplification efficiency by non-radiative relaxation [17]. Despite

the high chemical durability and superior chemical resistance of SiO_2 glasses, fluorescence studies are limited to only a few transitions owing to their higher phonon energies. Rather, non-oxides hosts (e.g., fluoride and chalcogenide glasses) exhibit more metastable states and undergo transparencies beyond 2000 nm wavelength [18]. New glass compositions with heavier glass ions and weaker bond strengths are presently suitable glass hosts for RE-doped optical devices, particularly for RE such as Pr^{3+}, which displays fast non-radiative relaxation paths in oxides [19]. Glasses with lower phonon energy, such as fluoride, chalcogenide, or tellurite glasses, are prone to crystallize and thus have proved hard to make in fibers with low optical loss.

Among the different glass, oxide and non-oxide systems, transparent glass-ceramics (GC) offer remarkable features to the field of photonics. Glass-ceramics are a class of hybrid materials consisting of nanocrystallites embedded in a glass matrix. Transparency is a key property, in particular for dielectric optical waveguides and optical fibers, and the effect of the nanocrystals activated by RE ions on the spectroscopic properties overcomes largely those of RE ions in a glass [20, 21]. Moreover, the transparent glass-ceramics still retains the properties of a glass and can be processed and shaped by techniques used for glasses. Among the various techniques used to fabricate optical planar waveguides and photonic devices, sol-gel process with top-down and bottom-up approaches demonstrated to be a suitable route to do it [5, 10, 22]. A high doping level of RE ions can be achieved by sol-gel process. Despite the presence of hydroxyl groups (OH) of inherent character in sol-gel silicate glasses, which are extremely effective at quenching excited RE ions [3, 23], even for a few hundred ppm of OH, sol-gel is a powerful technology in the development of glasses containing RE for various types of applications.

2. Sol-gel glass: the solid with a liquid background

The rapid cooling of some molten materials (e.g., SiO_2, BeF_2, B_2O_3, As_2O_3, P_2O_5, and GeO_2) [24] has become the traditional way to make glass, an inorganic material of fusion that has cooled to an amorphous solid without crystallization. So, unlike crystals, a glass lacks long-range order. The crystallization can be avoided when the cooling is fast, and so the viscosity of the molten liquid increases so much that the atomic *rearrangement* becomes difficult and the material becomes amorphous, which is a solid without long-range periodic order, which means that the spatial arrangement of atoms and ions does not exhibit a three-dimensional periodicity and the long-range order of the crystalline state. Nevertheless, glasses do not necessarily have to be formed from rapid melt cooling. In the mid-nineteenth century, the sol-gel process emerged as an innovative choice for glassmaking, using as an alternative to the traditional method of melting, a technique of chemical synthesis in aqueous media, very effective in the preparation of glasses at low temperatures [10]. Sol-gel glasses are prepared usually using alkoxides and soluble salts (precursors) by heat treatments at low temperatures [10]. The precursors are selected molecules that contain the elements of the future glass network and allow its formation by chemical reactions in liquid medium, silicates, aluminates, phosphates, and so on. Although the term alkoxide has been firstly applicable to products obtained from alcohols, by replacing the hydrogens of the hydroxide groups with a metal (Ti, Zr,

etc.) or non-metal (Si, Ge, etc.), their use was generalized to compounds of the type $M(OR)_n$ wherein M represents the metal or nonmetallic atom and R the organic radical [10]. Because many alkoxides are soluble in a wide range of organic solvents, especially alcohols, they are extremely versatile and so are the most commonly used in the preparation of inorganic solids. However, there are many other precursors with interest in the sol-gel process, namely carboxylates ($M(OCOR)_n$), acetylacetonates ($M(CH_3COCHCOCH_3)_n$), and inorganic salts such as nitrates and chlorides. These two last kinds of precursors are a very common to introduce RE ions in the glass network. As an example, Er^{3+} ions can be easily added as an ethanol solution of $Er(NO_3)_3{\cdot}9(H_2O)$ or $ErCl_3{\cdot}6(H_2O)$. The traditional sol-gel process may be exemplified in the case of the preparation of silica glass [10]. So the process one needs an alkoxide precursor of M(OR)n type, for example, TEOS (M = Si; R = C_2H_5), water, an alcoholic solvent and a catalyst, acid or base [10]. The process begins with the hydrolysis of the alkoxide, which allows the formation of monomers (hydroxide *species*, M-OH), which are small solid fragments with a great potential to bind to each other during the condensation reactions (aggregates of several monomers) [10]. These fragments, initially very small (≪100 nm), progressively increase in size until they occupy all the available volume of the solution, forming a three-dimensional (3D) network corresponding to the final structure of the glass. The process is called sol-gel because at a given moment a transition from a "*sol*" phase to a "*gel*" phase occurs [10]. Let's see some basic details: (1) the hydrolysis reaction consumes the initially added water, allowing the condensation reaction to occur, producing water as well. This water will be consumed again by the hydrolysis until all the alkoxides are hydrolyzed, which means that alkoxide ions are gradually replaced by OH^- ions. During this process, modifications of the polarity and viscosity of the medium occur, which give rise to a "*sol*"; (2) the condensation reactions continue until all monomers capable of binding are exhausted, which naturally lead to the formation of species of the —M—O—M— (or $(—Si—O—Si-)_n$) type which remain "immobilized" at one stage, highly viscous, called "*gel*"; and finally (3) after drying the "gel" (loss of solvent by evaporation) [10], a high porosity solid is obtained which must be further densified (at a temperature close to glass transition temperature, T_g) to become a solid, dense glass. A brief look on the process is shown in **Figure 1**. We can define a sol-gel glass saying that it is solid with a liquid background! In fact, the liquid undergoes an evolution over time and reaches the equilibrium when it becomes structurally a solid. This approach enables to make of an interested analogy between the sol-gel process and *Darwin's Theory*. Charles Darwin was an English naturalist who published in 1859 the well-known book *Origin of Species*, explaining how living species beings adapt continually to the environment, assuring the survival of their descendants by reaching equilibrium. Through the sol-gel processing, a true evolution of species occurs and so the "*sol*" could well be called *Darwin's liquid*, since it reaches the "perfection" when a 3D cross-linked network is attained and becomes a glass. As in *Darwin's Theory*, the sol-gel evolution does not happen by chance, rather it is stimulated by several imbalances in the *alkoxide-water-alcohol-acid* system, such as changes in pH, viscosity, temperature, and so on, which force precursors to adapt continuously in the middle: *dimer* → *chain* → *ring* is the progression in the polymerization process. Each monomer bond that is established is a tiny evidence of *Species Evolution* in this process!

Sol-gel synthesis is nowadays used to produce glasses with a variety of compositions that are technically difficult or even impossible to produce by melting. Some binary and

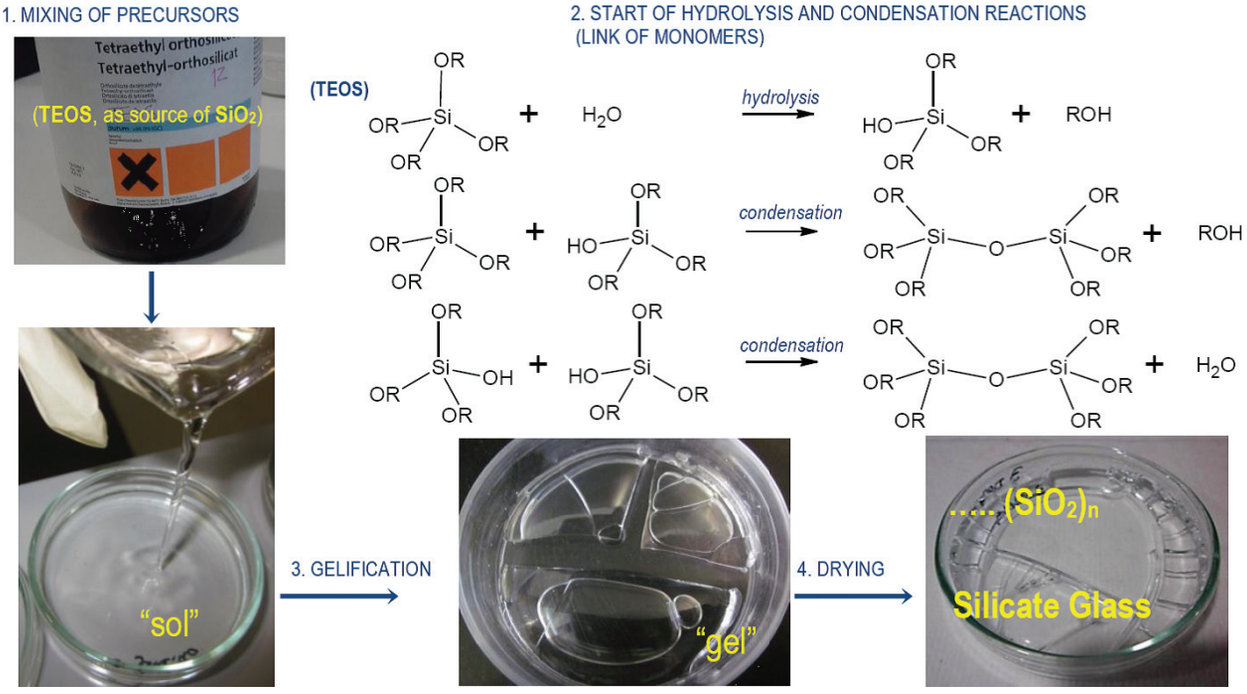

Figure 1. Scheme of the evolution sol → gel → glass.

multicomponent oxide systems exhibit liquid-liquid immiscibility and tend to phase separate in a short range of compositions and temperatures and thus can be successfully obtained by sol-gel. This process does indeed offer great possibilities to tailor the preparation of highly homogeneous glasses, such as RE-doped glasses. When RE ions are hosted by glasses, they exchange the network cation or they act as network modifiers [25]. It is therefore expected that the RE ions will favor non-bridging oxygen sites in the gel as the solvent is expelled. In addition, sol-gel method also offers the possibility of obtaining glassy coatings on silicon substrates to achieve planar waveguides [5]. A method of depositing thick sol-gel coatings is illustrated in **Figure 2a**.

Planar waveguides have a central rectangular region of higher refractive index n_1 (core) that is surrounded by other region, which has a lower refractive index n_2, as shown in **Figure 2b**. The deposition of multi-nano-silica-based glass layers on silicon substrates to obtain thick (micron) planar waveguides (which can later be coupled to external guide fibers) can be done by simple and multilayer deposition techniques (spin-coating and/or dip-coating) [26] of sol-gel solutions, allowing coatings with thickness and controlled refractive index. Indeed, by varying the precursor ratios in the sol, glasses of a wide range of compositions, and thus a desired refractive index, can be achieved; for example, SiO_2/TiO_2 of different molar ratios allows a wide index range from 1.46 to over 1.6. For waveguides, a bilayer is formed: a lower index buffer, n_2 (e.g., SiO_2) of sufficiently thick to prevent leakage of guided light into the substrate, and a higher index guiding layer, n_1 (e.g., SiO_2/TiO_2).

The refractive index in thin films containing SiO_2 (n ~1.46) increases linearly with the relative TiO_2 content, generally ca. 0.07 per 10 mol% of TiO_2 [27]. The guiding layer may also be doped with a functional material; for example, RE can be added to the sol through a variety of

http://dx.doi.org/10.5772/intechopen.68534

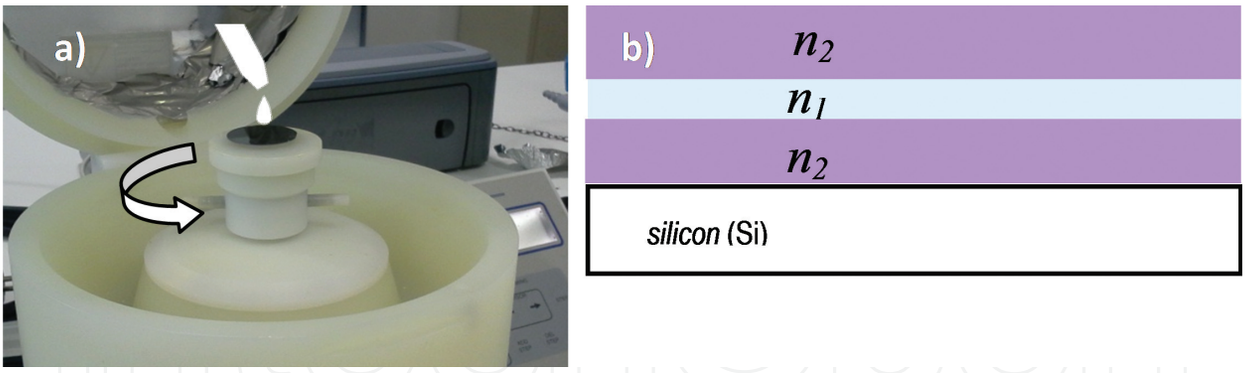

Figure 2. (a) Spin-coating process and (b) planar waveguide structure (on silicon substrate). n, refractive index; $n_1 > n_2$ (for total internal reflection).

precursors. A few drops of "*sol*" are spun to a thin layer on the Si-substrate, where upon the solvent evaporates and the condensation is speeded, giving a partially dense "*gel*" coating. This coating is subsequently heated to burn away remaining organics groups and achieves complete densification; repetition of this process can produce a multi-micron coating. Fully dense and homogeneous layers can be formed at relatively low temperatures, and the molecular structure formed chemically in the sol is maintained in the final glass. Thus, RE ions could be incorporated in the sol by condensation reactions, at the required high doping levels, and that this structure could be maintained in the glass. At low concentrations, the RE ions can be distributed homogeneously in an SiO_2 glass network with the formation of Si—O—RE structure. However, with an increasing concentration, due to close proximity between the RE ions and oxygen ions (~1.5–2 nm), RE—O—RE clusters may eventually form [28]. Sol-gel offers some advantages over FHD and CVD, namely greater flexibility in host glass composition and the possibility of homogeneously incorporating RE by chemical reaction in the sol. However, its major drawbacks are the excessive shrinkage of a wet gel upon drying which leads often to the crack, in particular of large monolithic pieces, inhomogeneous linkage during sol formation (in multicomponent glasses) due to differential reactivity of alkoxide precursors, and the presence of residual porosity and OH groups. Measurements of wavelength shape, intensity, and width of optical spectra and of excited state lifetimes can reveal the existence of RE clustering and the presence of OH in the neighborhood of the RE ions. Indeed, lifetime may be shortened if the hydroxyl content is not reduced to very low concentrations. The annealing process removes any excess water and OH groups as well as creating a dense, amorphous product, the sol-gel glass. However, the removal to a few ppm levels requires special chemical treatments with reactive gases like $CC1_4$, $C1_2$, and so on [29]. Residual porosity must also be removed by densification to prevent internal fluorescence quenching.

3. Basic principles of fluorescence: specificities of sol-gel glasses

Among usual forms of light interaction with matter (absorption, reflexion, etc.), fluorescence is a very special one that can be regarded as a source of light, or, in other words, a phenomenon in which a material radiates light (emission) at longer wavelength after a brief interval (termed

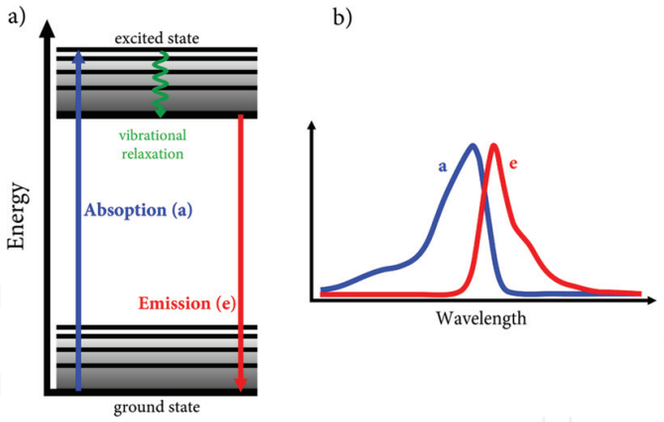

Figure 3. (a) Fluorescence scheme; (b) absorption spectrum (a) plus emission spectrum (e).

fluorescence lifetime), as a result of absorption of shorter wavelength. Fluorescence in optical glass is generated by the presence of RE ions. When these active ions are directly excited by incoming energy, the electron on it absorbs energy and is raised to an excited state (**Figure 3a**). The excited state returns to the ground state by emission of light of longer wavelength (**Figure 3b**). This behavior (absorption by short wave light, emission of longer wave light) is named "*fluorescence*" [30].

The processes that occur between the absorption and fluorescence emission of light are generally illustrated by the Jablonski [31] diagram. Indeed, **Figure 3a** shows a very simplified Jablonski diagram where the transitions between states are represented as vertical lines.

Following light absorption, emission usually occurs. Prior to emission, a rapid relax to the lowest vibrational level takes place, called vibrational relaxation, which is a non-radiative transition [32]. This process yields a relaxed excited state from which fluorescence emission originates. The fluorescence results from combined rates of radiative and non-radiative processes from a metastable excited state to the ground state (e.g., Er^{3+} transition $^4I_{13/2} \rightarrow {}^4I_{15/2}$ at 1550 nm). Radiative decay (W_R) deals with photon emission during de-excitation processes, while in a non-radiative decay (W_{NR}) the excited electronic states relax by energy dissipation via thermal processes such as vibrational relaxation and collisional quenching. Because RE ions may interact with vibrations of the matrix, either intrinsic or due to impurities (defect vibrations), non-radiative decay rates (W_{NR}) can occur. The total decay rate of an excited state (W_T) is then given by

$$W_T = W_R + W_{NR} \tag{1}$$

where

$$W_{NR} = W_{MP} + W_{ET} + W_{CR} + W_{OH} \tag{2}$$

W_{MP}, W_{ET}, W_{CR}, and W_{OH} are the rates of multiphonon decay, energy transfer, cross relaxation, and decay due to water (OH groups) in glasses, respectively. The W_{OH} component for the non-radiative decay cannot be neglected for sol-gel glasses [23] since being a very

effective fluorescent-quenching mechanism of transferring energy to OH groups, by non-radiative multiphonon relaxation. Moreover, W_{MP} can be relevant because it deals with the phonon density of states, which is high in solids, so the high-energy losses come from the highest-energy phonons of the matrix [14, 30, 32]. Oxide glasses have superior W_{MP} due to their higher network vibrational frequencies, when compared to halides and chalcogenides. For glasses, in particular for SiO_2-based glasses, the vibrations causing multiphonon relaxation are the high frequency, localized stretching modes of their oxygen-based Si—O—Si structural bonds. W_{ET} strongly depends on the average distance and thus the concentration of active ions (due to ion-ion interactions). This process is particularly important when the RE ion concentration increases (up to concentration quenching). Moreover, cross-relaxation or cooperative up-conversion processes [32] can occur due to concentration quenching. The fluorescence efficiency is degraded if the non-radiative decay is similar to the radiative one. This means, in practice, there is a significant reduction in the quantum yield (η) of RE ions and a shortening of the measured metastable level lifetime (τ_{meas}). Quantum yield is the number of emitted photons relative to the number of absorbed (pump) photons. W_R and W_{NR} both depopulate the excited state through emission, and hence the η is given by the ratio between the radiative decay rate and the total (radiative + non-radiative) decay rate, according to Eq. (3):

$$\eta = \frac{W_R}{W_R + W_{NR}} \tag{3}$$

Glasses with the largest quantum yields, approaching unity, display emissions with major fluorescence intensity; the fluorescence lifetime (τ_{meas}), instead, refers to the average time a population of N-active ions stays in its excited state before emission and is usually determined by using fluorescence decay measurements [30]. The temporal evolution of the population of excited states follows Eqs. (**4**) and (**5**) [30]:

$$\frac{dN(t)}{dt} = -W_T N(t) \tag{4}$$

where

$$N(t) = N_0 e^{-W_T t} \tag{5}$$

N_0 is the density of excited ions at $t = 0$, just after the pulse light is absorbed. The de-excitation process can be experimentally observed by analyzing the temporal decay of the emitted light, $I(t)$, as shown in **Figure 4a**. Therefore, the fluorescence decay is exponential given by Eq. (6) [30]:

$$I(t) = C \times W_R N(t) = I_0 e^{-W_T t} \tag{6}$$

where C is a constant of proportionality and $I_0 = C \times W_R \times N_0$ is the intensity at $t = 0$. As shown in **Figure 4a**, τ_{meas} is the measured lifetime that also corresponds to the time in which the emitted intensity decays I_0/e.

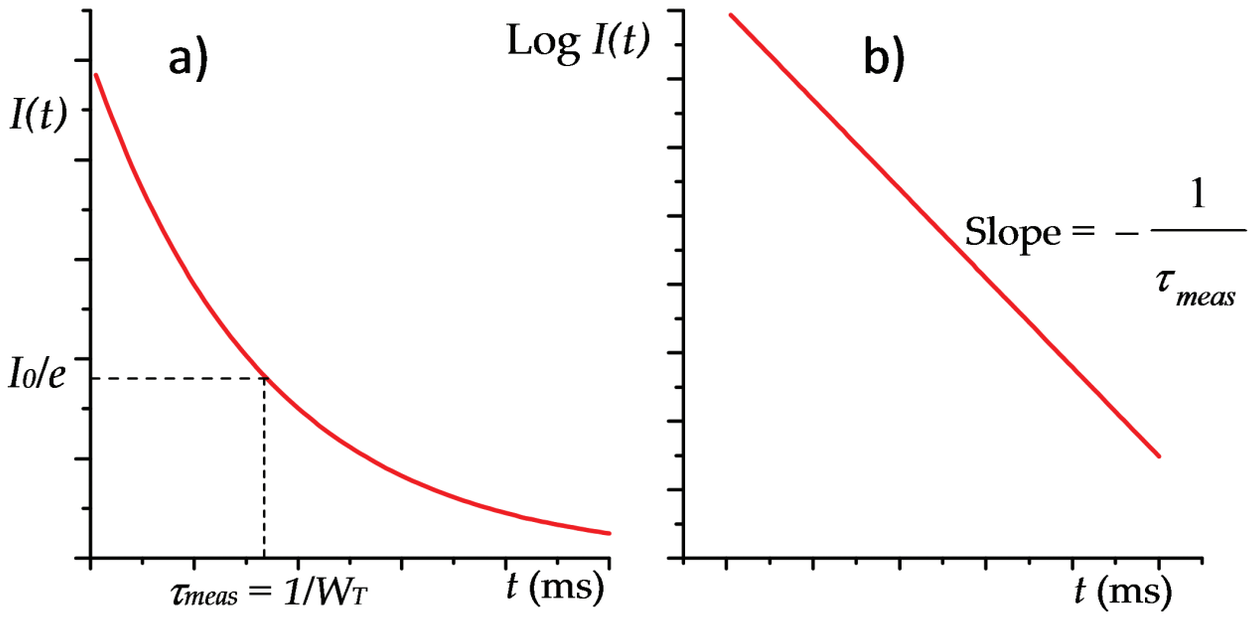

Figure 4. (a) Fluorescence decay; (b) linear plot of $I(t) = I_0 e^{-W_T t}$.

The lifetime, τ_{meas}, also corresponds to the slope of the linear plot of Eq. (6), exhibited in **Figure 4b**. Therefore, Eq. (1) can be rewritten by Eq. (7):

$$\frac{1}{\tau_{meas}} = W_R + W_{NR} = \frac{1}{\tau_R} + W_{NR} \tag{7}$$

where τ_R is the value of the lifetime before the non-radiative processes has been reached (also named radiative lifetime or excited state lifetime). Hence, η calculated from Eq. (3) can also be given by Eq. (8):

$$\eta = \frac{W_R}{W_R + W_{NR}} = \frac{\tau_{meas}}{\tau_R} \tag{8}$$

Because the fluorescence intensity is directly proportional to the number of molecules in the excited state, lifetime measurements can be done by measuring fluorescence decay after a brief pulse of excitation [30]. **Figure 5** shows the fluorescence decay of Ho^{3+} ($^5I_7$) at 2000 nm, fitted with a single exponential curve, measured for Ho^{3+}-doped sol-gel glass. However, in this case, visual inspection indicates a poor fit to the experimental data, confirmed by an R^2 of 0.97506. Therefore, in such cases, the fluorescence decay profile can be better fitted with the double exponential function, composed by the sum of two exponentials, as shown in Eq. (9):

$$I(t) = A_1 e^{(-t/\tau_1)} + A_2 e^{(-t/\tau_2)} \tag{9}$$

where τ_1 and τ_2 are often defined as the fast and slow components of a fluorescence decay profile. In RE-doped glass-ceramics (GCs), the decay curves of the luminescence are usually adjusted to a double exponential. As previously mentioned, sol-gel GCs are obtained from a glass matrix when an accurate thermal treatment is applied [20, 21]. During this thermal process,

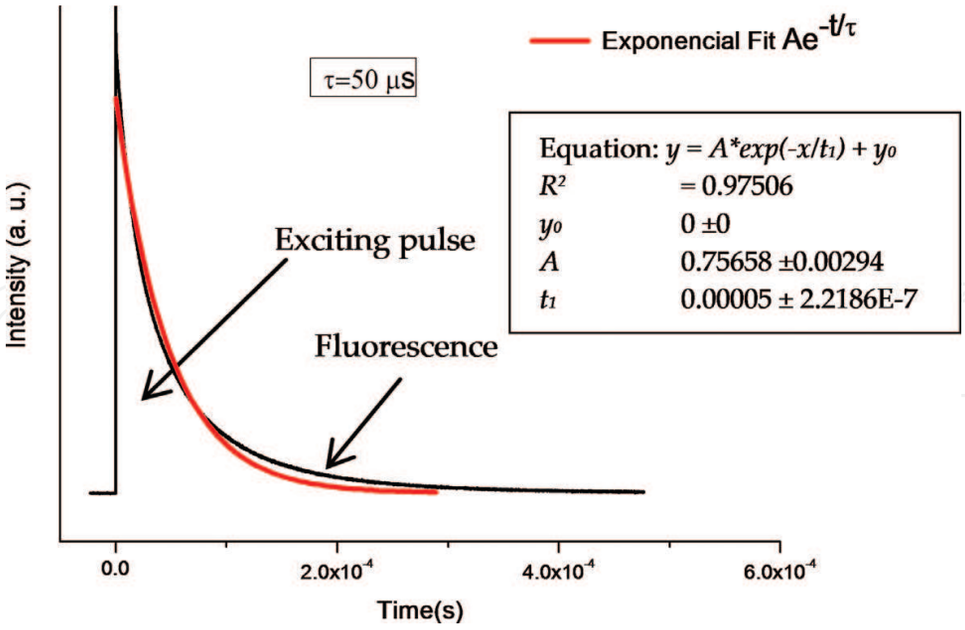

Figure 5. Decay curve of the holmium fluorescence ($^5I_7$) in a sol-gel glass; fit by single exponential decay.

nanocrystals precipitate into the host matrix and the RE dopants divide into the nanocrystalline and glassy phases.

Some of the ions predominantly doping the nanocrystals and another part remain in the vitreous state, so the average distance between them increases reducing concentration quenching. This approach has been widely reported in the literature [33], assigning the lifetime of the remaining RE ions in the vitreous phase to the decay of the fast component, while the slow component will correspond to the ions within the crystalline environment. For the multi-exponential decay is usually defined a mean life, which is given by Eq. (10) [34]:

$$\tau_{av} = \frac{A_1\tau_1^2 + A_2\tau_2^2 + A_3\tau_3^2}{A_1\tau_1 + A_2\tau_2 + A_3\tau_3} \tag{10}$$

where A_3 and τ_3 come from Eq. (9), duly adapted to three components. In the absence of a host (the nanocrystals) in the vicinity of the RE ions to optimize spectroscopic properties (e.g., phonon energies, etc.), RE ion-doped sol-gel glasses have normally ions concentration, which is relatively high and so the mean distance between two of them may be small enough to allow a non-negligible probability of energy interaction. In fact, if one of the ions is excited it can transfer its energy to a nearby one. Frequently, the excitation is also transferred from a sensitizer ion (e.g., Yb^{3+}) to another active ion (Er^{3+}). The influence of the concentration quenching on the reduction of RE ion quantum yield was first evidenced by Förster and Dexter [35, 36] who showed that the electronic energy transfer probability strongly depends on the ion-ion distance through an empirical criterion applied to a microscopic system of two ions interacting among them. The empirical formula, which relates the measured lifetime to the ion concentration, c, is

$$\tau_{meas} = \frac{\tau_{co}}{1 + \left(\frac{c}{Q}\right)^{p}} \tag{11}$$

where τ_{co} is the lifetime in the limit of zero concentration (c~0) and Q is the quenching concentration, at which $\tau_{meas} = \tau_{co}/2$. Energy transfer significantly affects the luminescence properties of a material. However, in some particular cases, energy transfer processes occurring between RE ions could be advantageous, as those between Yb^{3+} and Er^{3+} ions, which are widely used for optical amplification at 1550 nm. In such systems, the pump radiation (at 980 nm) is strongly absorbed by Yb^{3+} ions, which acts as the sensitizer. Subsequently, the Yb^{3+} ions efficiently transfer their energy to the Er^{3+} ions at ground state by emitting light at 1550 nm. This process is known as down-conversion [34, 37] because high-energy excitation photons are transformed to lower-energy photons. Rather, up-conversion (UC) is the most common sense of this phenomenon whereby photons of lower energy are absorbed by a material, to be re-emitted as a higher-energy photon. An important feature is that materials can be tuned to respond to NIR (low energy) to emit at high energies at visible wavelengths range. Up-conversion laser emission can be easily achieved, for instance, in pairs Er^{3+}-Yb^{3+} or Ho^{3+}-Yb^{3+} co-doped glasses, where high-energy photons (green or blue light) can be obtained from red or infrared light (low-energy photons) [38]. A typical experimental setup to record UC visible emission spectra is shown in **Figure 6**. The UC visible spectrum of Er^{3+}-Yb^{3+} doped sol-gel glass excited at 980 nm, relax emitting light in the visible; the $^2H_{11/2}/^4S_{3/2} \rightarrow {}^4I_{15/2}$ green emission lines are clearly dominant, as shown in **Figure 6**. Various combinations with different RE ions and appropriate thermal treatments offer the possibility to optimize the fluorescence intensity, lifetime, and the energy transfer between doping ions. From the various fluorescence-quenching processes, some of them have a special significance in glasses made by sol-gel which are (1) concentration quenching via cross-relaxation, (2) non-radiative vibrational excitation of hydroxyl groups (OH), and (3) multiphonon relaxation due to impurities (defects vibrations). These mechanisms decrease fluorescence efficiency [34]. Moreover, it was shown that RE-host interactions result from defects (porosity and/or passive crystallites dispersed in matrix), expressed by an intensity decrease in the fluorescence emission; symmetry factors that arise from host nature (amorphous or crystalline), expressed by the character of the lifetime decay curve, and cross-relaxation, expressed by the broadening/narrowing (shape) of a specific transition [15]. All of these processes depend on the type and composition of the glass used. The high concentration of OH groups that remain in sol-gel glasses decreases the fluorescence quantum yield and shortens lifetimes of RE ions in glasses [3, 34] affecting negatively the optical device performance.

OH quenching arises from the residual water, solvents, and silanol groups (Si—OH) of the early stages of sol-gel glasses. This leads to an enhancement of non-radiative decays due to the coupling between the RE states and the high vibrational energy of OH (3200 cm^{-1}) [3, 4].

Annealing the doped gels changes the local environment of the RE ions, which results in changes in the fluorescence emission shape [15].

http://dx.doi.org/10.5772/intechopen.68534

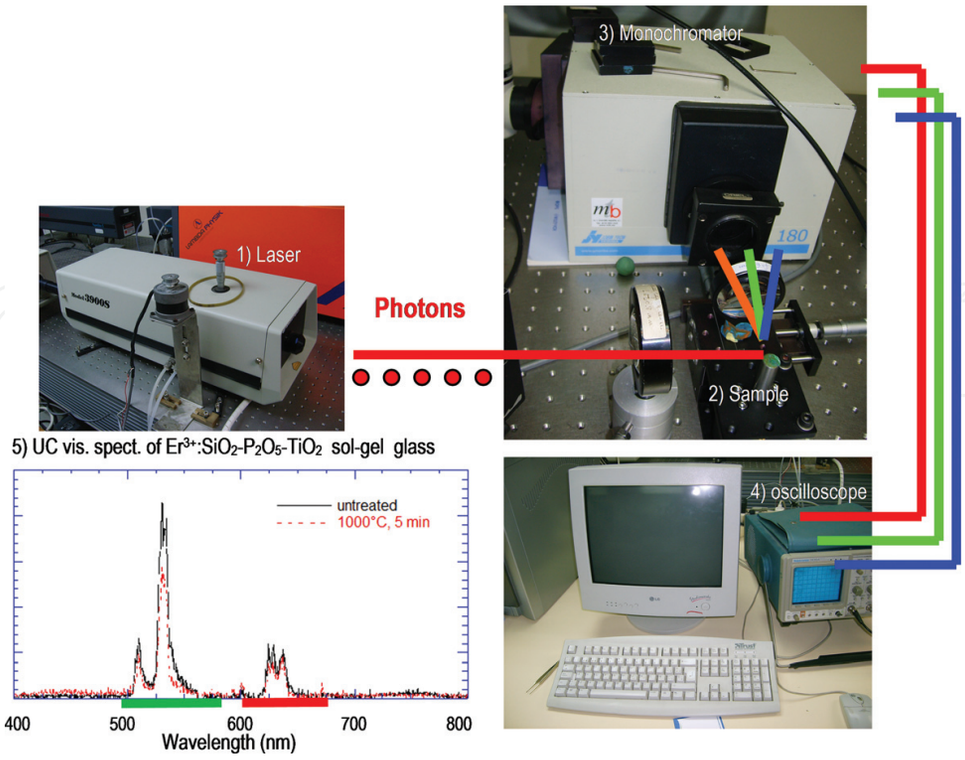

Figure 6. Experimental setup to record UC emission spectra: (1) excitation source (laser); (2) sample (Er^{3+}: SiO_2-P_2O_5-TiO_2 sol-gel glass); (3) monochromator/PMT; (4) oscilloscope (to acquire the signal); and (5) sample UC spectrum.

4. The 4f-4f transitions of rare earths and intensity probabilities

The REs are a group of 15 chemical elements from the Lanthanide series (atomic number, Z, ranging from 57 to 71, at the sixth row of the periodic table), starting in lanthanum (La) and ending in lutetium (Lu), which exhibit similar chemical behavior and high stability in their triply ionized form (3+). When incorporated in crystalline or amorphous hosts, the RE maintains their most stable ionized form [39]. All REs have the general configuration $[Xe]4f^n5s^25p^6$ where [Xe] is the electronic configuration of Xenon and *n* represents the number of internal electrons (the optical active electrons) in level *4f* [39]. Their most remarkable characteristic is the partially filled *4f* shell that is shielded from external fields by the $5s^2$ and $5p^6$ electrons, allowing a 4f electrons behavior similar to that exhibited in a free RE ion [39]. The energy levels of RE are therefore largely insensitive to the environment in which they are placed [39–41]; the effect of the static crystal field of the environment becomes very weak, causing only small host-induced splitting [3, 41]. The crystal field is the electric field interaction between the RE ion and surrounding ions of the host matrix. An inherent characteristic of the RE ions is that their optical transitions occur within the 4f shell reducing the influence of the host lattice on the wavelengths, bandwidths, and cross sections of the relevant optical transitions, which correspond therefore to weak, sharp absorption and emission lines [3]. In a crystal, each ion in the lattice is affected by the same intensity of the crystalline field, whose influence on the electronic

transitions leads to narrow bands, resembling those of the free ions. In glasses, however, the bands are considerably broadened [41]. Each RE ion is affected by a different crystalline field and therefore exhibits unlike Stark levels. Each ion has its own absorption and emission spectra and its own radiative decay rates. Therefore, the glass fluorescence properties can be viewed as a kind of average of all ion fluorescent behaviors. Thus, there is a site-to-site variation in the energy levels of these ions and hence in their radiative and non-radiative transition probabilities lead to the band broadening. Although the shielding of the 4f shell means that the RE ion energy levels are largely insensitive to the host, Stark splitting broadens the levels as a result of the crystal field. Stark splitting is observed for RE ions in glasses, as a result of a large quantity of sites that differ from each other in the number and position of the surrounding anions [41]. In order to characterize the energy levels associated with the electronic levels 4f, the Russell-Saunders notation (or LS-coupled states) is often used, represented as $^{2S+1}L_J$ [41]. This notation couples the angular momenta (L) and spins of the valence electrons (S) to a total angular momentum J. The energy levels are then identified according to the $^{2S+1}L_J$ notation, where the term $2S + 1$ is the spin multiplicity and $L = 0,1,2,3,4,5,6$ … correspond to S,P, D,F,G,H,I…, respectively. The free Er^{3+} ion, for instance, has an electron configuration $4f^{11}$ for which the lower term is $^4I_{15/2}$, and the first excited multiplet $^4I_{13/2}$, which is about 6500 cm^{-1} higher than $^4I_{15/2}$. So when $L = 6$ (state I) and $S = 3/2$ (the total spin quantum number for $4f^{11}$ electrons can be 3/2, with three unpaired, or 1/2, with only one unpaired) [39], J may assume several terms (J multiplets) as $^4I_{15/2}$, $^4I_{13/2}$, $^4I_{11/2,}$ and $^4I_{9/2}$ which correspond to the lowest-energy states of the Er^{3+} ion. In 1964, Dieke published the energy diagram of all trivalent RE ions within $LaCl_3$, knowing as "*Dieke diagram*." Due to the negligible influence of the host lattice on the energy levels, the diagram is applicable to RE ions in any host matrix [42], including glass, crystals, and glass-ceramics, very useful to estimate the symmetry of the environment where the ion is placed. The absorption spectrum of Er^{3+}:80SiO_2 20TiO_2 (mol%) sol-gel glass is shown in **Figure 7**. From optical absorption, it is possible to determine energy levels of the RE ions and identify them through Dieke diagram, as shown in the inset of **Figure 7**. The absorption transitions between specific Stark components of different J multiplets can be detected at room temperature as separate peaks in RE-doped crystals, but not in glasses [3, 41], where a broad band overlaps them. In 1962, Judd and Ofelt proposed a theory [43, 44] to estimate transition probabilities, or radiative decays (W_R). This theory offers an alternative approach to obtain radiative transition probability of all excited states, radiative lifetime, and quantum yield by calculating phenomenological parameters (Ω_i, i = 2, 4, 6), known as the Judd-Ofelt (JO) parameters, from experimentally observed absorption data. In addition, this theory can also be used to predict oscillator strengths (f) of and branching ratios (β) [30]. This f can be expressed under specific conditions as a function of Ω_i whose values are directly influenced by the host matrix [45] and provide a quantitative measure of the asymmetry of the local crystal field of RE ion. The parameter Ω_2 is sensitive to the covalent bonding between the RE ions and the ligands anions, for example, RE-O bonding [45], which is an indication of the asymmetry of the local environment of the RE sites. This means that it is small for ionic host material, for example, fluoride glasses, while it is large for covalent host materials, such as silicate glasses. Moreover, for a glass co-doped with more than one type of RE ions, for example, Yb^{3+} and Er^{3+}, the possibility of a reduction on the number of non-bridged oxygens to coordinate with Er^{3+} ions is high, which can cause the decrease of the covalency between Er-O oxygen bonds, and, therefore, decrease Ω_2. On the other hand, Ω_4 and Ω_6 reveal

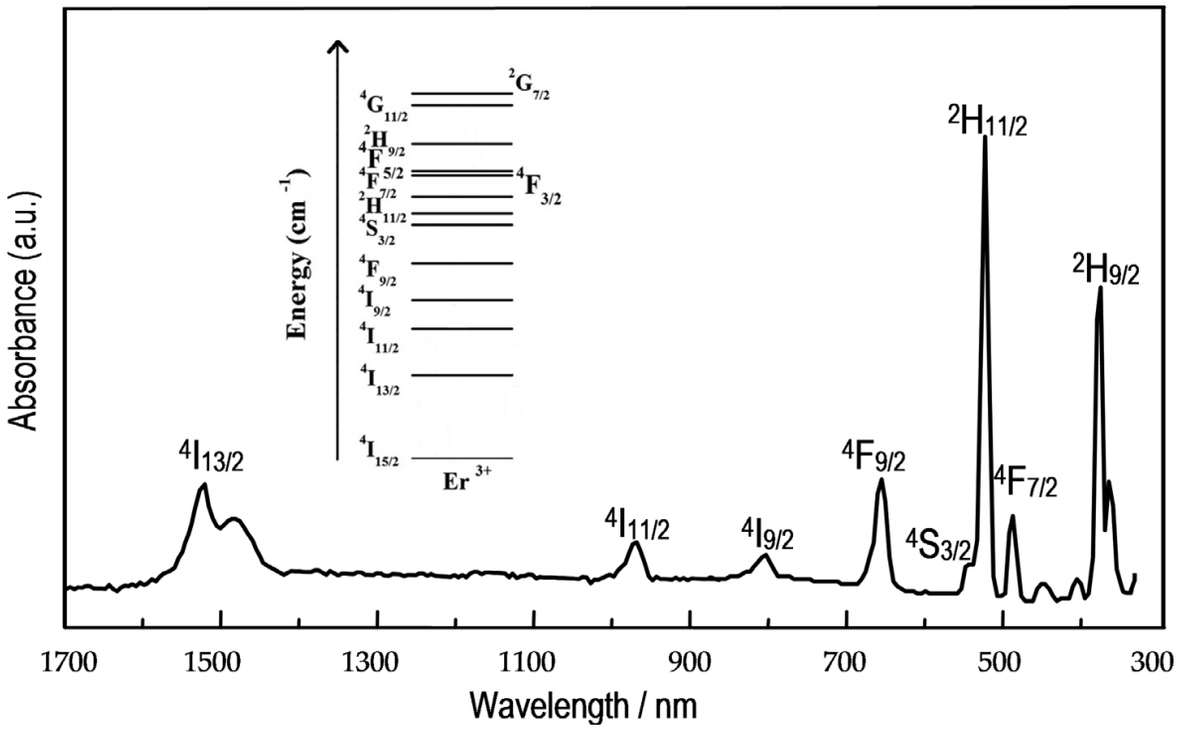

Figure 7. Absorption spectrum of Er^{3+}-doped $80SiO_2$-$20TiO_2$ glass. Inset: schematic energy level diagram of Er^{3+} ion (from Dieke diagram).

broad properties of the host glass such as rigidity and viscosity. Moreover, the ratio Ω_4/Ω_6 is a spectroscopic indicator of the quality of the parameter used to predict the strength of the radiative emission of the first transition (e.g., $^4I_{13/2} \rightarrow {}^4I_{15/2}$: 1550 nm in Er^{3+}: SiO_2 glass). For sol-gel glasses, the calculated Judd-Ofelt parameters are average values from a multiplicity of sites for RE ions in different environments. From the absorption spectrum (**Figure 7**), the experimental oscillator strengths (f_{exp}) of the electronic transitions can be calculated using the expression:

$$f_{\exp} = \frac{mc}{\pi e^2 N} \int \frac{2.303 OD(\upsilon)}{d} d\upsilon \tag{12}$$

where m and e are the electron mass and charge, respectively, c is the light speed, N is the concentration of absorbing ions, υ is the light frequency, $OD(\upsilon)$ is the optical density, which is proportional to the absorption coefficient (α), and d is the thickness of the sample. The f_{exp} values obtained using Eq. (11) and the experimental absorption spectrum can therefore be used to obtain the JO parameters [46]. The experimental oscillator strength, f, is fitted to the theoretical expressions in the frame of the JO theory using a statistical least-square algorithm or chi-squared methods. The radiative emission probabilities between two electronic states can be calculated, according to the JO theory, if they are known.

5. Tailoring sol-gel-derived SiO_2 glassy optical waveguides

Nowadays, great attention still is given to the development of efficient and compact planar optical waveguides, with active (doped) and/or passive (undoped) purposes, for integrated

optical devices [4]. Light propagation in passive waveguides depends strongly on the layer structure and morphology, whereas propagation losses or attenuation must be kept as low as possible. Several factors are considered to disturb the light propagation [4, 47]: (1) absorption losses (AL_1) due to light absorption in the glass waveguide (due to electronic (UV-visible) absorption at the Urbach edge and vibrational (IR) absorption at the multiphonon edge); (2) scattering losses (SL_1) due to refractive index fluctuations; (3) absorption losses (AL_2) by impurities like OH; and (4) scattering losses (SL_2) due to the imperfection of the waveguide structure such as defects or surface roughness.

Porosity, dopants, and crystalline phases within the volume of the waveguide cause volume scattering while surface scattering loss can be significant for rough surfaces. Indeed, these kinds of imperfections can appear in sol-gel glasses-derived waveguides in the form of porosity, cracks, polycrystalline phases, dust contamination, and so on, as a result of deposition operation. However, particularly for sol-gel-derived waveguides, some of the imperfections such as pores and cracks are almost inevitable, as shown in **Figure 8**. Moreover, the porous removal requires high annealing temperatures to densify the waveguides, and thus cracks can occur from internal stress [10].

The principal types of defects that may cause scattering losses in sol-gel waveguides are shown in **Figure 9**.

They can be classified as textural defects (cracks, pores, dust, and surface roughness), compositional defects (nanocrystallites and discontinuous refractive index), or structural defects (thickness changes, internal stress and interaction between film and substrate, etc.). The size and the optical properties of these imperfections control their degree of contribution for the scattering loss with the operational wavelength.

Furthermore, light scattering tends to increase with λ^{-1}. According to Rayleigh's law, when the imperfection size is smaller than λ, the light diffusion is roughly proportional to λ^{-4}.

Therefore, the longer wavelength range produces a weaker propagation loss. Silica glass is transparent in NIR and exhibits a non-negligible attenuation. Alternatives to this material are heavy metal fluorides (ZBLAN) glasses, transparent in the mid-infrared (MIR) wavelength range. For SiO_2 glasses, here are two λ_{min} which correspond to the communication channels at 1310 and 1550 nm, respectively. The minimum absorption depends on the vibrational modes (intrinsic "phonons") of the atomic network and shifts to higher wavelengths with increasing atomic mass. However, although the theoretical predictions are notably more favorable to ZBLAN, in practice, these materials are difficult to obtain either in fiber or in waveguide configuration. SiO_2 gives high gain levels per unit length in silica-based waveguides and thus remains a very attractive optical glass even though their emissions from the energy levels of RE dopants are decidedly linked to be non-radiative than radiative ones. This is because the phonon energy of the sol-gel silica glass is higher than most of other glasses. One way to overcome this problem is to use a low vibrational energy matrix with heavy oxides such as GeO_2 or TeO_2. While sol-gel is well suited to oxides, it is still little studied for other systems. Despite this, germanium sulfide films, based on sol-gel preparation and dip or spin coating, have achieved waveguiding features [48]. Glass hosts typically exhibiting higher RE solubility

http://dx.doi.org/10.5772/intechopen.68534

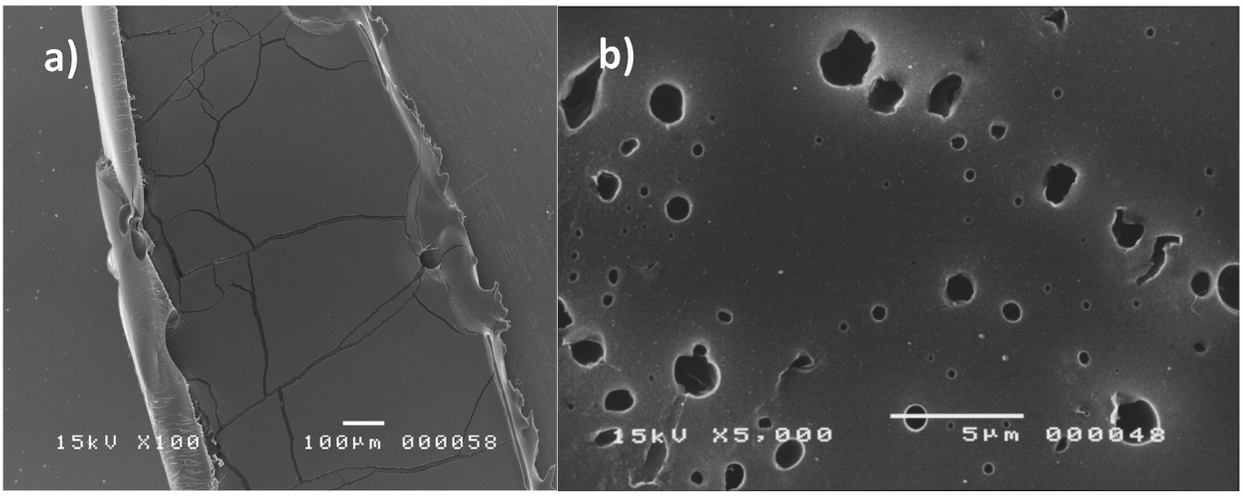

Figure 8. SEM images of Er^{3+}:SiO_2-TiO_2-Al_2O_3 sol-gel glasses: (a) at 500°C thermal treated and (b) as deposited, where defects as micro-cracks and pores can be observed, respectively.

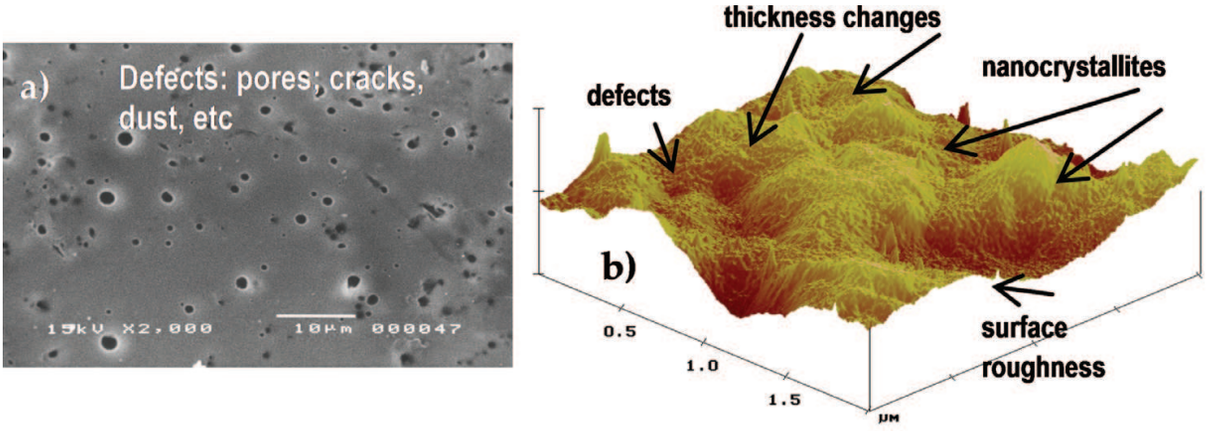

Figure 9. Different textural, compositional, and structural defects on sol-gel thin films of Er^{3+}:SiO_2-TiO_2-P_2O_5: (a) SEM images of the thin film annealed at 200°C, exhibiting a highly porous surface; (b) AFM of the thin film annealed at 700°C exhibiting a singular morphology and an average roughness.

and lower phonon energies are highly favorites to develop active waveguides as they result in longer excited state lifetimes of RE emissions. However, beyond the energy lost to host glass through lattice vibrations, there are two critical additional quenching mechanisms in sol-gel glasses: (1) energy transfer to hydroxyl (OH) groups owing to the some fundamental vibrations (between 2700 and 4000 nm) which are unavoidable due to the use of water and alcoholic solvents during the preparation process and (2) energy transfer between RE ions due to cluster formation even at lower concentration (concentration quenching). Indeed, a fluorescence intensity decrease is commonly attributed to cross-relaxation mechanisms of RE ions in clustering RE—O—RE bonds [27]. The Er^{3+} fluorescence emission of the $4I_{13/2} \rightarrow {}^4I_{15/2}$ transition in silicate glasses exhibits a characteristic shape, as depicted in **Figure 10** [21], which can, however, change its intensity due to non-radiative rates related to ion clustering [27] but also related to the presence of pores and passive or not optically active crystalline phases (e.g., anatase or rutile in the case of SiO_2-TiO_2 glasses) within the matrix [21].

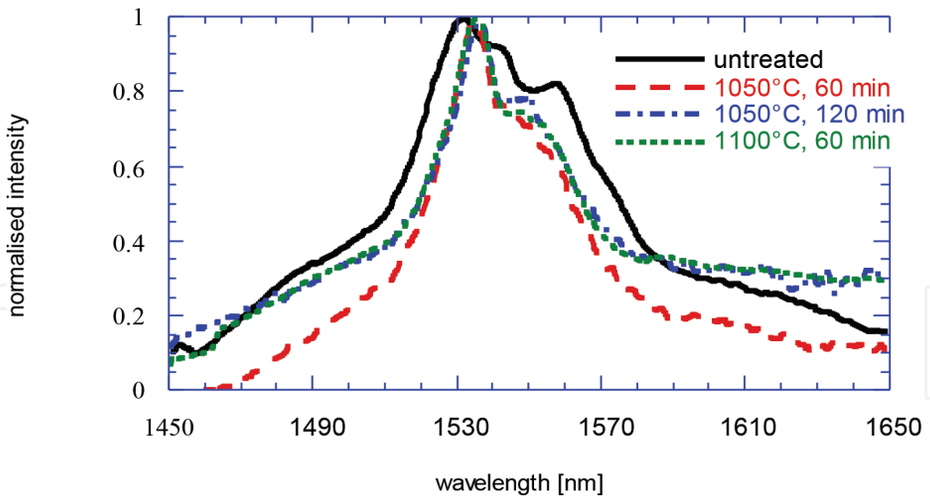

Figure 10. Erbium fluorescence in Er^{3+}:SiO_2-TiO_2 films for different heat treatments.

Fourier transform infrared spectroscopy (FTIR) is one of the most popular analytical techniques used to study the microstructural evolution of sol-gel glasses as a function of temperature and synthesis parameters. The FTIR spectrum of $80SiO_2$-$20TiO_2$ glass, as soon after deposition (wet), is shown in **Figure 11a**. The broad peak around 3300 cm^{-1} is the fundamental stretching vibration of OH group, which reveals, as expected, the presence of hydroxyl groups in the gel, the *fingerprint* of sol-gel glasses. Hydroxyl concentrations, in ppm, can be determined using the Beer-Lambert law [49]. Moreover, the peak around 1600 cm^{-1} is assigned to the bending mode of the H_2O molecule. The other bands relate to characteristic vibrations of the glass structure itself, namely the dominant band at 1080 cm^{-1} with a shoulder at 1185 cm^{-1} is assigned to asymmetric stretching vibrations of the tetrahedral SiO_4^- unit (Si—O—Si); the peak arising at 465 cm^{-1} results from rocking vibrations of Si—O—Si bonds and the band around 980 cm^{-1} is assigned as stretching vibration of silanol groups, Si—OH, owing to non-bridging oxygen which overlaps stretching vibrations of Si—O—Ti bonds at ~950 cm^{-1}. This latter is usually taken as an indicator of the degree of condensation revealing the homogeneity in the glass network, whereas the 1080 cm^{-1} band is indicative of SiO_2-rich regions. The effect of temperature on OH band, exhibiting a pronounced lowering at temperatures higher than 600°C, is clear in **Figure 11b**. In fact, the OH-stretching vibration in Er^{3+}-doped silicate glasses affects the fluorescence decay at 1550 nm because only two OH vibrations are enough to bridge the gap of ~6500 cm^{-1} between the $^4I_{15/2}$ and the $^4I_{13/2}$ states. The presence of OH species in the matrix also leads to reduction of quantum yield at the first excited state of Er^{3+} ions. However, there are chemical limitations to the solubility of RE in various glassy materials which become even more significant with an increase in the concentration of RE ions. This limitation is explained by a disparity in size and valence between the RE ions and the SiO_2 network components. Hence, an effective way to increase the amounts of RE ions in a SiO_2 glass and avoid clustering effects is the addition of co-doping oxides, such as P_2O_5 or $A1_2O_3$ [28, 50].

When a non-glass-forming oxide such as Al_2O_3 is added to an SiO_2 glass, the Si—O—Si bond is broken, which leads to the formation of two types of oxygen: the oxygen that is attached to

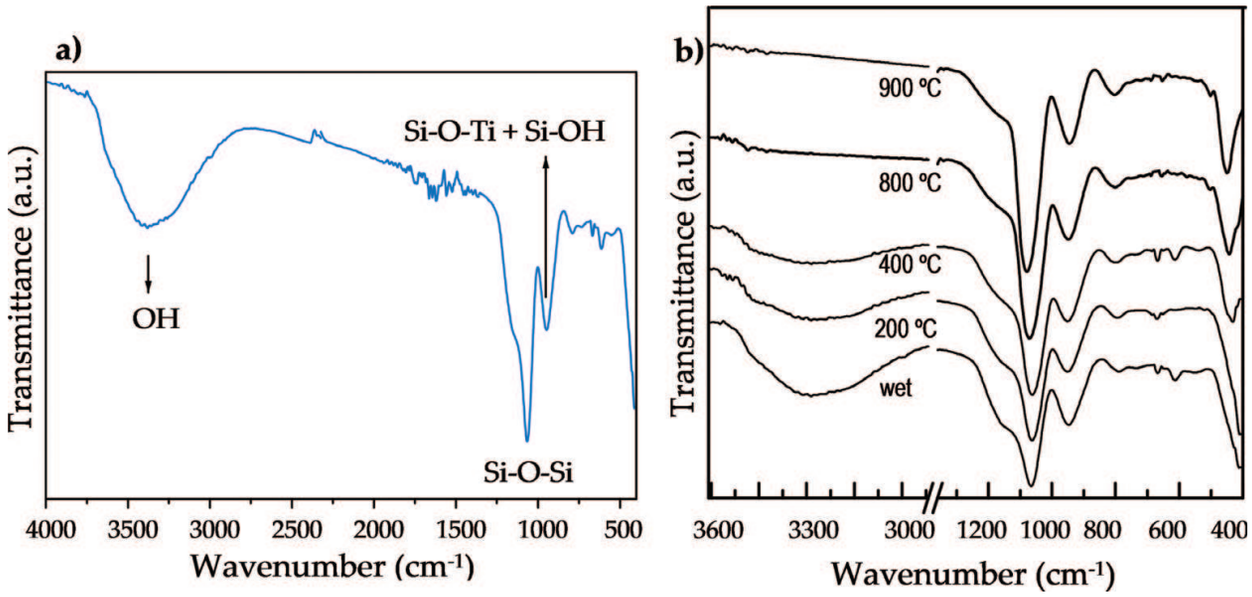

Figure 11. (a) Transmission IR spectrum for the composition $80SiO_2$-$20TiO_2$ immediately after deposition; (b) FTIR spectra of Er^{3+}:$80SiO_2$-$20TiO_2$ glasses heat treated up to 900°C.

two Si, called the bridge oxygen (BO) and the other, which is connected to one Si, called non-oxygen bridge (NBO). Each RE ion solubilized in the glass matrix needs three NBOs to compensate the 3+ charges. Since RE ions cannot induce the necessary coordination number of NBO, therefore the RE clustering becomes energetically more favorable to share the limited number of NBO. Rather, the Al^{3+} ions embedded in the silicate glass matrix can be incorporated in two local bonding configurations such as tetrahedrally coordinated ($AlO_{4/2}$), as a network former or octahedrally coordinated ($AlO_{6/2}$), as a network modifier. Therefore, Al—O—RE bonds are formed instead of RE—O—RE ones, thus increasing the RE solubility. Also, the phonon energy of the Al—O—Si bonds is smaller than that of Si—O—Si vibration. Besides, P_2O_5 is also used as co-doping agent to improve the fluorescent properties of RE ions in sol-gel glasses [16, 21]. In fact, the breaking up of the RE—O—RE regions and formation of RE—O—P or RE—O—Al bonds is highly likely and allows, for example, Nd^{3+} contents as high as 7 wt% before phase separation or clustering are observed [51]. FTIR and X-ray photoelectron spectroscopy (XPS) can provide valuable information about bonding configuration of glasses and a quantitative estimation of the Si—O—NBO species and thus contribute to improve the design of new active waveguides. **Figure 12** shows the FTIR spectra of $80SiO_2$-$20TiO_2$-xP_2O_5 (x = 0, 5, 10 mol%) sol-gel films. The growing incorporation of phosphorus in the SiO_2-TiO_2 matrix leads to a decrease of the band at 950 cm^{-1} which reveals an inhibition of the formation of Si—O—Ti^{4+} terminal species in favor of Si—O—P—O —Ti^{4+} species [28]. XPS measurements allow estimation of the concentrations of the different types of oxygen atoms present in the Si—O—Ti, Si—O—P and Si—O—Al bonding sequences. The O 1s XPS spectra for $80SiO_2$-$20TiO_2$-xP_2O_5 (x = 0–15 mol%) sol-gel films are shown in **Figure 13**, which displays the existence of different chemical environments for the oxygen atoms. Based on the electronegativities of the different elements involved (O, Ti, Si, and P), the individual bond types are assigned as follows: 530.7 eV, to Ti—O—Ti bonds; 531.5 eV, to Si—O—Ti bonds; 533.8 eV, to Si—O—Si bonds; and 534.4 eV, to Si—O—P bonds, since higher the ionic character of the

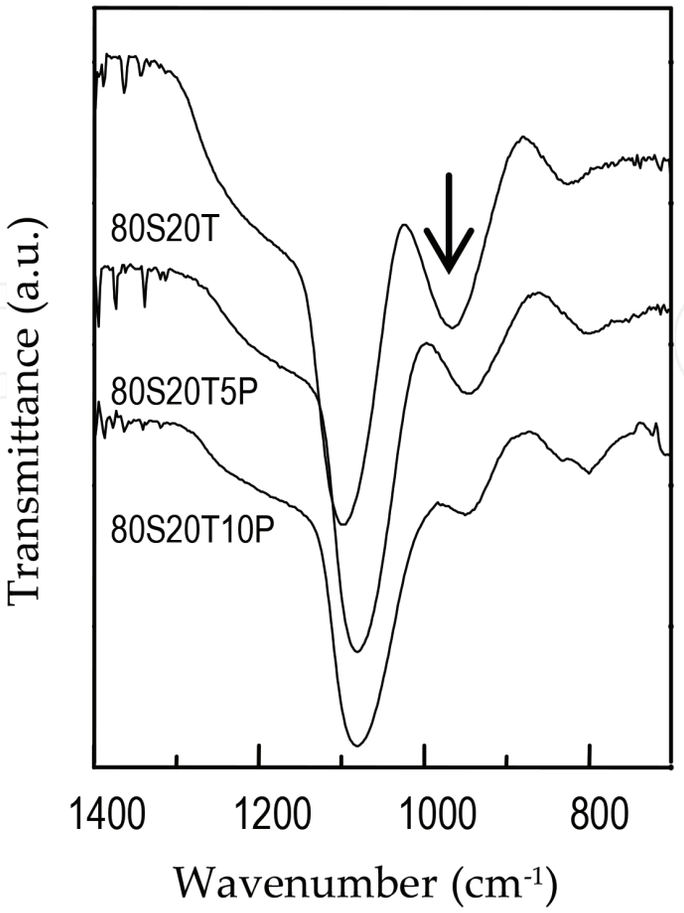

Figure 12. FTIR spectra of $80SiO_2$-$20TiO_2$-xP_2O_5 (x = 0–10 mol%) glasses heat treated at 900°C, 2 min.

bonds, lower is the O 1s binding energy. The fraction of oxygen atoms in Si—O—Ti and Si—O—P bonds can be calculated from the measured areas of each of the two components relative to the total O 1s peak area.

The influence of the high vibrational energy of SiO_2-based glasses on non-radiative relaxation can be minimized by the incorporation of RE ions into nanocrystals with low-energy phonons dispersed in the matrix. This ordered environment would avoid any RE ions clustering. The interest demonstrated in recent years by nanocomposite GC is due to the possibility of creating a low-vibrational energy neighborhood around RE ions leading to a higher luminescent efficiency. Nevertheless, a nanocrystal larger than 10–15 nm drastically increases the propagation losses. This alternative becomes especially interesting for the following reasons: (1) a host material (the nanocrystal) is used in the vicinity of the RE ions in order to optimize the spectroscopic properties; (2) the matrix is still a suitable fiber junction material, with superior processing and high stability. The optical properties of waveguides doped with nanocrystals (fluorescence spectrum, fluorescence life, and optical losses) were found to be basically dependent on the following parameters: (a) nature of the nanocrystalline phases obtained; (b) crystallite sizes; (c) volume fraction of crystalline phases dispersed in the amorphous matrix; and (d) residual concentration of RE ions retained in the amorphous matrix. The XRD patterns of $80SiO_2$-$20TiO_2$-$ErO_{1.5}$ sol-gel thin films in **Figure 14** show different crystalline phases. At 1000°C, only anatase

http://dx.doi.org/10.5772/intechopen.68534

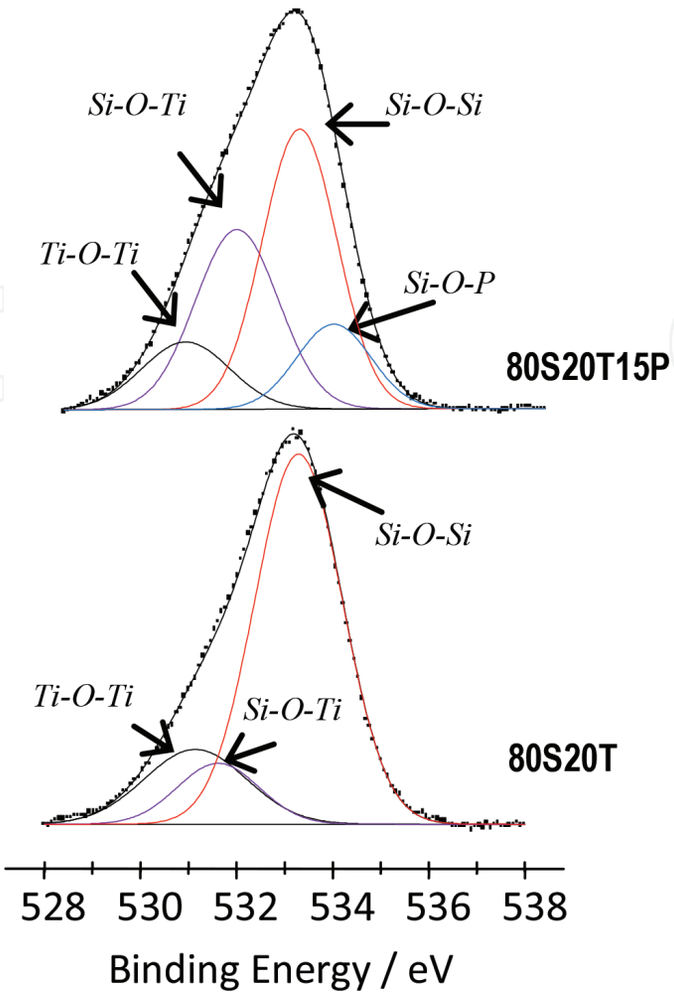

Figure 13. Deconvoluted spectra of O 1s $80SiO_2$-$20TiO_2$-xP_2O_5 (x = 0–10 mol%) glasses.

phase, one of the crystalline polymorphic forms of TiO_2, among rutile and brookite, is evidenced by its main peak at 25.28, which corresponds to (101) plane. By increasing the annealing temperature, the decomposition of anatase phase took place and a transition from anatase to rutile crystalline phase occurs.

The main peak of the film annealed at 1050°C is at 27.44, which corresponds to rutile (110) plane. The active phase $Er_2Ti_2O_7$ precipitates together with rutile at 1100°C. Both anatase and rutile are passive phases that can damage the fluorescence quantum yield by scattering losses. In fact, high treatment annealing lowers the OH content but can increase the losses scattering from non-optical crystals such as rutile.

The interest in $Er_2Ti_2O_7$ is obviously because Er^{3+} ions are inserted in a locally well-ordered phase thus giving relatively sharp photoluminescence emissions in a wide range of spectral bands from infrared to the blue region.

Results indicated clearly that the luminescence was significantly improved while erbium was present in the form of $Er_2Ti_2O_7$ crystallites dispersed in an amorphous matrix [21]. When the content of Er_2O_3 (the most usual erbium precursor) greatly exceeds the solubility limit of the

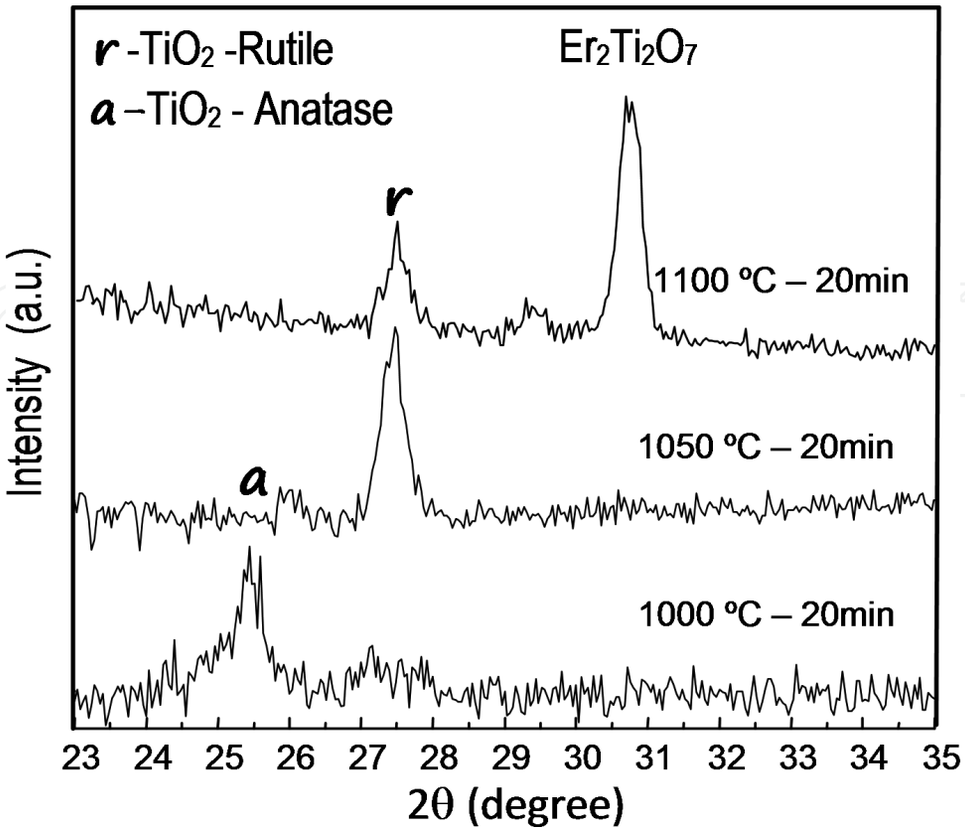

Figure 14. X-ray diffraction pattern of $80SiO_2$-$20TiO_2$-$ErO_{1.5}$ waveguides annealed at 1000, 1050, and 1100°C.

glass, it reacts almost entirely with P_2O_5 forming $ErPO_4$ (EPO) crystallites. In the SiO_2-TiO_2-P_2O_5 system, the $ErPO_4$ particles are crystallized during the glass-annealing process. It has been shown that $ErPO_4$ nanocrystals resulted in an increase in the fluorescence lifetime at 1550 nm greater than 200% with a maximum value of 9 ms [21]. **Figure 15** shows the room temperature fluorescence spectra relative to the $^4I_{13/2} \rightarrow {}^4I_{15/2}$ obtained upon 514.5-nm excitation, for $80SiO_2$-$20TiO_2$-$ErO_{1.5}$ waveguides. All the spectra exhibit a main emission peak at 1530 nm with a shoulder at

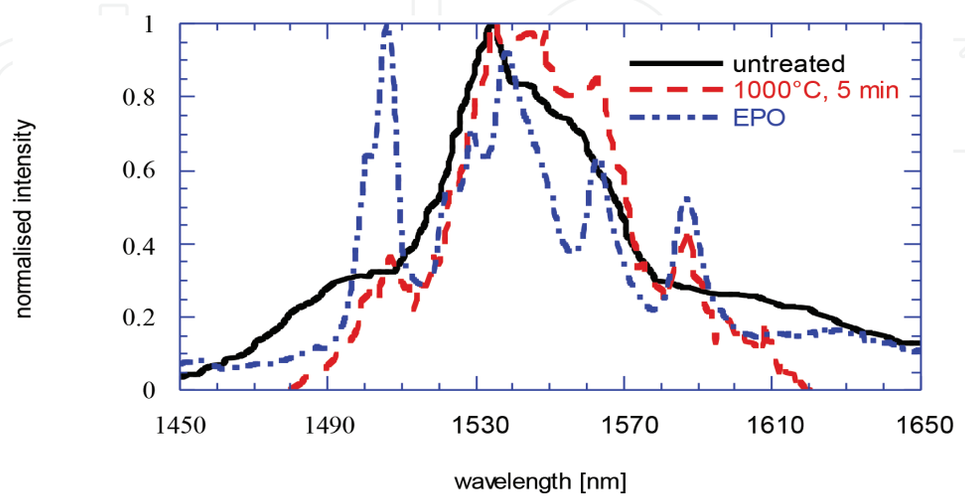

Figure 15. Fluorescence spectrums relative to the $^4I_{13/2} \rightarrow {}^4I_{15/2}$ transition of the Er^{3+} ions for $80SiO_2$-$20TiO_2$-P_2O_5-$ErO_{1.5}$ waveguides at different heat treatments, upon excitation at 514.5 nm.

about 1550 nm. $ErPO_4$, on the other hand, emits a well-detectable fluorescence band around 1535 nm, with four peaks due to the Stark splitting of the $^4I_{13/2}$ level in the crystalline compound.

6. Conclusions

Glass-integrated optics is controlled by oxide glasses, in part because of advantages of production techniques. At present, the Er^{3+}-doped optical silicate glass is a very important light-amplifying element. However, non-oxides are receiving increasing interest for optical applications. Their low phonon energies make them useful for RE doping for lasers and amplifiers, particularly for doping with Pr^{3+} which have rapid non-radiative relaxation rates in oxides. A suitable approach to improve fluorescence lifetime of RE ion-doped glasses is to shield ions from the glass matrix in a local environment, such as a nanocrystallite, allowing optical properties of the host glass to be maintained. For the future, sol-gel has high potential for optical devices. A deep knowledge about materials physics and quantum optics is therefore essential to achieve these challenges.

Acknowledgements

The authors gratefully acknowledge the financial support from (1) FEDER, through Programa Operacional Factores de Competitividade—COMPETE and Fundação para a Ciência e a Tecnologia—FCT, by the project UID/FIS/00068/2013 and (2) Government of the Azores (DRCT - Programme PRO-SCIENTIA, Ref. M3.3.c/Edições/009/2017). The authors also wish to thank Dr. F. Rivera-López (ULL) for providing images used in this manuscript.

Author details

Helena Cristina Vasconcelos[1,2,3]* and Afonso Silva Pinto[3]

*Address all correspondence to: helena.cs.vasconcelos@uac.pt

1 Biotechnology Centre of Azores (CBA), Azores University, Ponta Delgada, Açores, Portugal

2 Centre of Physics and Technological Research (CEFITEC), FCT/UNL—Department of Physics, Quinta da Torre, Caparica, Portugal

3 Faculty of Science and Technology, Azores University, Ponta Delgada, Açores, Portugal

References

[1] Righini JC. 25 years of integrated optics: where we are and where we will go. Proc. SPIE. 2212, Linear and Nonlinear Integrated Optics, Giancarlo C. Righini, David Yevick, Editors, 2. (1994) DOI: 10.1117/12.185098

[2] Rimoldi, B. (2016) Principles of Digital Communication: A Top-Down Approach, Published by Cambridge University Press, United Kingdom. https://doi.org/10.1017/CBO9781316337387

[3] Digonnet MJF. Rare Earth Doped Fiber Lasers and Amplifiers. 2nd ed. New York, NY: Marcel Dekker Inc.: 1993. DOI: 10.1201/9780203904657

[4] Righini GC. Passive and active glasses for integrated optics. In: Mazzoldi P, editor. From Galielo's Ochialino to Optoelectronics. Singapore: World Scientific; 1993. pp. 272-294. DOI: 10.1604/9789810213329

[5] Orignac X, Almeida RM. Silica-Based Sol-Gel Optical Waveguides on Silicon in IEE Proceedings—Optoelectronics. 1996;**143**(5):287–292. DOI: 10.1049/ip-opt:19960834

[6] Colinge J-P. Silicon-On-Insulator Technology: Materials to VLSI. Boston, MA, USA: Kluwer Academic Publishers; 2004. DOI: 10.1007/978-1-4757-2611-4

[7] Hu H, Ricken R, Sohler W, Wehrspohn RB. Lithium niobate ridge wave-guides fabricated by wet etching. IEEE Photonics Technology Letters. 2007;**19**:6. DOI: 10.1109/LPT.2007.892886

[8] Bindra KS, Bookey HT, Kar AK, Wherrett BS. Nonlinear optical properties of chalcogenide glasses: Observation of multiphoton absorption Applied Physics Letters. 2016;**79**:1939. DOI: http://dx.doi.org/10.1063/1.1402158

[9] Kawachi M. Silica waveguides on silicon and their application to integrated-optic components. M. Optical and Quantum Electronics. 1990;**22**:392. DOI: 10.1007/BF02113964

[10] Brinker CJ, Scherer GW. Sol-Gel Science-The Physics and Chemistry of Sol-Gel Processing. San Diego; Academic Press: 1990. DOI: 10.1002/adma.19910031025

[11] Kreibig U, Vollmer M. Optical properties of metal clusters. Spring Series in Materials Science. 1995;**25**:13–201. DOI: 10.1007/978-3-662-09109-8

[12] Diehl R. High-Power Diode Lasers: Fundamentals, Technology, Applications. Springer Berlin Heidelberg; 2000. ISBN: 978-3-540-66693-6, DOI: 10.1007/3-540-47852-3

[13] Snitzer E. Optical maser action of Nd^{+3} in a barium crown glass. Physics Review Letters. 1961;**7**:444. DOI: https://doi.org/10.1103/PhysRevLett.7.444

[14] Layne CB, Lowdermilk WH, Weber MJ. Multiphonon relaxation of rare-earth ions in oxide glasses. Journal of Material Science Letters. 1994;**13**:615. DOI: https://doi.org/10.1103/PhysRevB.16.10

[15] Vasconcelos HC, Meirelles MG, Rivera-López F. Erbium photoluminescence response related to nanoscale heterogeneities in sol-gel silicates. Journal of Rare-Earths. 2013;**31**:18-26. DOI: 10.1016/S1002-0721(12)60228-2

[16] Vasconcelos HC. The effect of PO2,5 and AlO1,5 additions on structural changes and crystallization behaviour of SiO_2-TiO_2 sol-gel derived glasses and thin films. Journal of Sol-Gel Science and Technology. 2010;**55**:126-136. DOI: 10.1007/s10971-010-2223-8

[17] Miniscalco WJ. Erbium-doped glasses for fiber amplifiers at 1500 nm. Journal of Lightwave Technologies. 1991;**9**:234-250. DOI: 10.1109/50.65882

[18] Santa Cruz P, Morin D, Dexpert-Ghys J, Sadoc A, Glas F, Auzel F. New lanthanide-doped fluoride-based vitreous materials for laser applications. Journal of Non-Crystalline Solids. 1995;**190**:238-243. DOI: 10.1016/0022-3093(95)00273-1

[19] Kenyon AJ. Recent developments in rare-earth doped materials for optoelectronics. Progress in Quantum Electronics. 2002;**26**:225-284. DOI: 10.1016/S0079-6727(02)00014-9

[20] Santana-Alonso A, Yanes AC, Méndez-Ramos J, del-Castillo J, Rodríguez VD. Sol–gel transparent nano-glass-ceramics comprising rare-earth-doped $NaYF_4$ nanocrystals. Physica Status Solidi (a). 2009;**206**:2249-2254. DOI:10.1002/pssa.200881717

[21] Strohhöfer C, Fick J, Vasconcelos HC, Almeida RM. Active optical properties of Er-containing crystallites in sol-gel derived glass films. Journal of Non-Crystalline Solids. 1998;**226**:182. DOI: 10.1016/S0022-3093(98)00365-2

[22] X. Orignac, D. Barbier. Potential for fabrication of sol-gel-derived integrated optical amplifiers. Proc. SPIE 2997, Integrated Optics Devices: Potential for Commercialization, Edited by S. Iraj Najafi and Mario Nicola Armenise, 271 (January 23, 1997); DOI:10.1117/12.264157

[23] Yan Y, Faber AJ, de Waal H. Luminescence quenching by OH groups in highly Er-doped phosphate glasses. Journal of Non-Crystalline Solids. 1995;**181**:283-290. DOI: 10.1016/S0022-3093(94)00528-1

[24] Rawson H. In: Glass Chemistry. Inorganic Glass-Forming Systems. London, UK: Academic Press; 1967. pp. 123-207. DOI: 10.1007/978-3-642-78723-2_7

[25] Weber MJ. Science and technology of laser glass. Journal of Non-Crystalline Solids. 1990;**123**(1–3):208-222. DOI: 10.1016/0022-3093(90)90786-L

[26] Scriven LE. Physics and applications of dip coating and spin coating. Materials Research Society Symposium Proceedings. 1988;**121**:717. DOI: 10.1557/PROC-121-717

[27] cbv Weisembach L, Zelinski BJ, O'Kelly J, Morreale J, Roncone RL, Burke JJ. The influence of processing variables on the optical properties of SiO_2-TiO_2 planar waveguides. SPIE. 1991;**1590**:50. DOI: 10.1117/12.50201

[28] McGahay V, Tomozawa M. Phase separation in rare-earth-doped SiO_2 glasses. Journal of Non-Crystalline Solids. 1993;**159**(3):246–252. DOI: 10.1016/0022-3093(93)90230-U

[29] Mukher Jee SP. In: Klein LC, editor. Sol-Gel Technology for Thin Films, Fibers, Preform, Electronics and Specialty Shapes. NJ: Noyes Publications; 1988. DOI: 10.1002/adma.19890010816

[30] García Solé J, Bausá LE, Jaque D. An introduction to the optical spectroscopy of inorganic solids. New Delhi, India: John Wiley & Sons, Ltd.; 2005. p. 283. DOI: 10.1002/0470016043.app3

[31] Jablonski A. Über den Mechanisms des Photolumineszenz von Farbstoffphosphoren. Journal of Physics. 1935;**94**:38-46. DOI: 10.1007/BF01330795

[32] Reisfeld R. Radiative and non-radiative transitions of rare-earth ions in glasses. Structure & Bonding. 1975;**22**:123-175. DOI: 10.1007/BFb0116557

[33] Haro-González P, Lahoz F, González-Platas J, Cáceres JM, González-Pérez S, Marrero-López D, Capuj N, Martín IR. Optical properties of Er^{3+}-doped strontium barium niobate nano-crystals obtained by thermal treatment in glass. Journal of Luminescence. 2008;**128**:908-910, 2008. DOI: 10.1016/j.jlumin.2007.12.014

[34] Lakowicz JR. Principles of Fluorescence Spectroscopy. 3rd ed. New York, NY: Springer; 2006. DOI: 10.1007/978-0-387-46312-4

[35] Förster T. Zwischenmolekulare Energiewanderung und Fluoreszenz, Annals in Physics. 1948;**2**:55. DOI: 10.1002/andp.19484370105

[36] Dexter DL. A Theory of Sensitized Luminescence in Solids, Journal of Chemistry and Physics. 1953;**21**:836. DOI: 10.1063/1.1699044

[37] Bo F, Céline P, Jean-Luc A, Xianghua Z, Xianping F, Hongli M. Near-infrared down-conversion in rare-earth-doped chloro-sulfide glass GeS_2-Ga_2S_3-CsCl: Er, Yb. Journal of Applied Physics. 2011;**110**(11):113107. DOI: 10.1063/1.3665638

[38] Orignac X, Barbier D, Du XM, Almeida RM, McCarthy O, Yeatman E. A Theory of Sensitized Luminescence in Solids, Optical Materials 1999;**12**(1):1–18. DOI: 10.1016/S0925-3467(98)00076-7

[39] Wybourne BG. Spectroscopic properties of rare earths. Physics Today. 1965;**18**(9):70. DOI: 10.1063/1.3047727

[40] Peacock RD, Nieboer E, Jørgensen CK, Reisfeld R. The intensity of lanthanide f↔f transitions. Structure and Bonding. 2007;**22**:83–122. DOI: 10.1007/BFb0116556

[41] Weber MJ. The Role of Lanthanides in Optical Materials. Report Number: LBL-37536. 1995. Available from: https://publications.lbl.gov/islandora/object/ir%3A102074

[42] Dieke GH. Spectra and Energy Levels of Rare-Earth Ions in Crystals. New York, NY: Wiley; 1968. DOI: 10.1119/1.1976350

[43] Judd BR. Optical Absorption Intensities of Rare-Earth Ions, Physics Review B. 1962;**127**: 750. DOI: 10.1103/PhysRev.127.750

[44] Ofelt GS. Intensities of Crystal Spectra of Rare-Earth Ions, Journal of Chemistry and Physics. 1962;**37**:511. DOI: 10.1063/1.1701366

[45] Jorgensen CK, Reisfeld R. Judd-Ofelt parameters and chemical bonding. Journal of the Less Common Metals. 1983;**93**(1):107–112. DOI: 10.1016/0022-5088(83)90454-X

[46] Lahoz F, Capuj N, Haro-Gonzalez P, Martın IR, Perez-Rodrıguez C, Caceres JM. Stimulated emission in the red, green, and blue in a nanostructured glass ceramics, Journal of Applied Physics. 2011;**109**:043102. DOI: 10.1063/1.3549157

[47] Almeida RM, Morais PJ, Vasconcelos HC. Optical loss mechanisms in nanocomposite sol-gel planar waveguides. Proceedings of the SPIE. 1997;**3136**:296–303. DOI: 10.1117/12.284127

[48] R. M. Almeida , J. Xu, Sol–Gel Processing of Sulfide Materials, Handbook of Sol-Gel Science and Technology, Published by Springer, pp 1–26, 2016. DOI: 10.1007/978-3-319-19454-7_11-1

[49] Davis K, Agarwal A, Tomozawa M, Hirao K. Quantitative infrared spectroscopic measurements of hydroxyl concentrations in silica glass. Journal of Non-Crystalline Solids. 1996;**203**:27–36. DOI: 10.1016/0022-3093(96)00330-4

[50] Almeida RM, Vasconcelos HC, Gonçalves MC, Santos LF. XPS and NEXAFS studies of rare-earth doped amorphous sol-gel films. Journal of Non-Crystalline Solids. 1998;**232–234**:65–71. DOI: 10.1016/S0022-3093(98)00545-6

[51] Bowron DT, Newport RJ, Rigden JS, Tarbox EJ, Oversluizen M. An X-ray absorption study of doped silicate glass, fibre optic preforms, Journal of Materials Science. 1996;**31**:485. DOI:10.1007/BF01139168

IntechOpen